# Orthogonal Self-Aligned Electroless Metallization by Molecular Self-Assembly

Peter K.-H. Ho,*,† Robert W. Filas, David Abusch-Magder, and Zhenan Bao*

*Bell Laboratories, Lucent Technologies, 600 Mountain Avenue, Murray Hill, New Jersey 07974*

*Received June 19, 2002. In Final Form: September 17, 2002*

A strategy for achieving orthogonal electroless metallization (i.e., formation of a metal pattern not overlapping and self-aligned with a first metal pattern) is described. The approach comprises molecular passivation of a first gold pattern with 1-hexadecanethiol (HDT), followed by priming of the $SiO_2$ substrate with (3-aminopropyl)triethoxysilane (APS) and activation with Pd(II) complexation to spatially direct electroless nickel metallization. Scanning electron microscopy indicates that the nickel nucleates on the gold sidewall and grows laterally over the dielectric but not over the gold surface. This confirms successful deactivation of the intrinsic catalytic activity of gold. Using this two-step orthogonal self-assembly of the molecular resist and primer, a lateral nickel metal pattern orthogonal and self-aligned to the first gold pattern with line width down to 10 $\mu$m has been demonstrated. The process can also be applied to curved and flexible substrates.

## Introduction

The ability to inexpensively define a lateral metal array pattern of dissimilar metals opens up new possibilities in nanoscience technologies as well as in conventional and unconventional electronics. Such metal arrays may be used, for example, in integrated lateral thermocouple junctions, photoresponsive arrays, lateral tunneling junctions, and microelectromechanical systems (MEMS) in which the metallurgical junctions are perpendicular rather than parallel to the substrate plane. Traditionally it is not trivial to define such lateral metal junctions because of the need for accurate pattern definition and registration across several mask layers.

We explore in this Letter the possibility of using self-assembly approaches to spatially direct an electroless metallization process, and we demonstrate the formation of self-aligned lateral micron-scale metal junctions in this way. Electroless metal (EM) deposition[1] has numerous advantages compared to vacuum-based processes for thin film metallization, including speed and the possibility of conformal coverage. For example, electroless Au metallization has been successfully employed to fabricate high-quality narrow gate contacts (ca. 300 nm) with unusually high aspect ratios onto GaAs metal-semiconductor field effect transistors.[2] EM deposition also enjoys several advantages over electrodeposition,[3] which requires conductive and relatively open substrates. In EM deposition, the metal ion to be deposited (e.g., Ni(II), Cu(II), Au(III), Ag(I), Pd(II), Co(II), or Rh(III)) is spontaneously reduced onto an appropriately surface-activated substrate in the EM bath. To achieve this, dielectric surfaces will usually have to be primed with a metallic Pd/Sn colloid before electroless deposition.[1] On the other hand, many clean metal surfaces including those of Au, Ag, Cu, Pd, Pt, and Co are themselves catalytic toward many EM systems.

To achieve the appropriate masking and priming, we used 2-D self-assembled molecular films in both roles as resist and primer. The unique properties of spontaneous molecular assemblies of thiols on Au, Ag, and Cu,[4−9] as well as of alkylsiloxanes on $SiO_2$,[10−17] have been well documented. Such self-assembled films are formed through a surface-specific self-limiting mechanism. The use of an alkanethiol film to protect an underlying Au substrate from cyanide etch was described by the Harvard group[18,19] and has since spawned vast amounts of literature in microcontact printing of circuits and devices.[20,21] The use of 2-pyridylethylsiloxane or 3-aminopropylsiloxane films to complex Pd(II) and activate the dielectric surfaces toward EM is also previously known.[22−24] We combined

* Correspondence should be sent to pkhh2@cam.ac.uk or zbao@lucent.com.

† Also at Department of Physics, University of Cambridge, Cambridge CB2 0HE, U.K.; and Department of Materials Science, National University of Singapore, Kent Ridge Crescent S119260, Singapore.

(1) *Electroless plating: fundamentals and applications*; American Electroplaters and Surface Finishers Society: Orlando, FL, 1990.

(2) Wada, S.; Tokushima, M.; Fukaishi, M.; Matsuno, N.; Yano, H.; Hida, H.; Maeda, T. *IEEE Trans. Electron Devices* **1998**, *45*, 1656−1662.

(3) Moffat, T. P.; Yang, H. *J. Electrochem. Soc.* **1995**, *142*, L220−222.

(4) Nuzzo, R. G.; Fusco, F. A.; Allara, D. L. *J. Am. Chem. Soc.* **1987**, *109*, 2358−2368.

(5) Porter, M. D.; Bright, T. B.; Allara, D. L.; Chidsey, C. E. D. *J. Am. Chem. Soc.* **1987**, *109*, 3559−3568.

(6) Bain, C. D.; Troughton, E. B.; Tao, Y.-T.; Evall, J.; Whitesides, G. M.; Nuzzo, R. G. *J. Am. Chem. Soc.* **1989**, *111*, 321−335.

(7) Laibinis, P. E.; Whitesides, G. M.; Allara, D. L.; Tao, Y. T.; Parikh, A. N.; Nuzzo, R. G. *J. Am. Chem. Soc.* **1991**, *113*, 7152−7167.

(8) Folkers, J. P.; Laibinis, P. E.; Whitesides, G. M.; Deutch, J. *J. Phys. Chem.* **1994**, *98*, 563−571.

(9) Delamarche, E.; Michel, B.; Kang, H.; Gerber, C. *Langmuir* **1994**, *10*, 4103−4108.

(10) Haller, I. *J. Am. Chem. Soc.* **1978**, *100*, 8050−8055.

(11) Netzer, L.; Sagiv, J. *J. Am. Chem. Soc.* **1983**, *105*, 674−676.

(12) Wasserman, S. R.; Tao, Y.-T.; Whitesides, G. M. *Langmuir* **1989**, *5*, 1074−1087.

(13) Balachander, N.; Sukenik, C. N. *Langmuir* **1990**, *6*, 1621−1627.

(14) Angst, D. L.; Simmons, G. W. *Langmuir* **1991**, *7*, 2236−2242.

(15) Brzoska, J. B.; Shahidzadeh, N.; Rondelez, F. *Nature* **1992**, *360*, 719−721.

(16) Parikh, A. N.; Allara, D. L.; Azouz, I. B.; Rondelez, F. *J. Phys. Chem.* **1994**, *98*, 7577−7590.

(17) Bierbaum, K.; Kinzler, M.; Wöll, C.; Grunze, M.; Hähner, G.; Heid, S.; Effenberger, F. *Langmuir* **1995**, *11*, 512−518.

(18) Kumar, A.; Biebuyck, H. A.; Abbott, N. L.; Whitesides, G. M. *J. Am. Chem. Soc.* **1992**, *114*, 9188−9189.

(19) Kumar, A.; Whitesides, G. M. *Appl. Phys. Lett.* **1993**, *63*, 2002−2004.

(20) Jeon, N. L.; Nuzzo, R. G.; Xia, Y.; Mrksich, M.; Whitesides, G. M. *Langmuir* **1995**, *11*, 3024−3026.

(21) Bao, Z.; Feng, Y.; Dodabalapur, A.; Raju, V. R.; Lovinger, A. J. *Chem. Mater.* **1997**, *9*, 1299−1301.

(22) Dressick, W. J.; Dulcey, C. S.; Georger, J. H., Jr.; Calabrese, G. S.; Calvert, J. M. *J. Electrochem. Soc.* **1994**, *141*, 210−220.

(23) Kind, H.; Bittner, A. M.; Cavalleri, O.; Kern, K.; Greber, T. *J. Phys. Chem. B* **1998**, *102*, 7582−7589.

10.1021/la0260988 CCC: $22.00 
Published on Web 11/01/2002

**Scheme 1. Schematic Diagram Showing Activation of the Dielectric $SiO_2$ Surface by Pd Clusters toward Catalytic Reduction of $Ni^{2+}$ Ions in the Presence of a Reducing Agent (Red) but Simultaneous Passivation of the Metallic Au Surface by an Alkanethiol[a]**

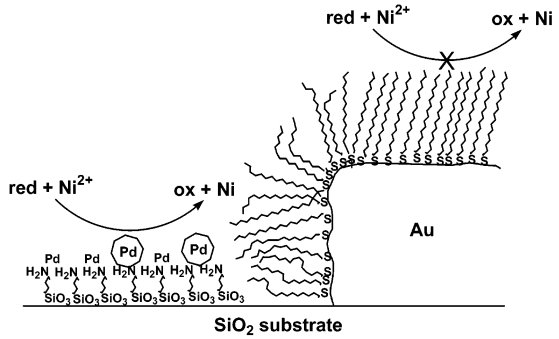


[a] This self-aligned orthogonal metallization leads to the formation of lateral metallic junctions.

these two key steps here and determined the experimental conditions for mutual compatibility so as to fabricate a lateral self-aligned heterojunction of two dissimilar metals of Au and Ni on Si (Scheme 1).

## Experimental Section

**Test Pattern.** Test comb array patterns with 800-$\mu$m-long and 10-$\mu$m-wide Au lines separated by exposed 20-$\mu$m-wide native-$SiO_2$ (14 Å) on a Si substrate were used. These were fabricated by standard lithography and lift-off of 90-nm-thick Au on 3-nm Ti films evaporated onto the substrate. Cleaning: The substrates were cleaned in an RCA recipe of 10:2:1 $H_2O/H_2O_2/NH_4OH$ at 70−80 °C for 5 min, which also removes surface Ti contamination. (*CAUTION*: Danger of explosion in contact with organics! *NOTE*: Prolonged treatment leads to undercutting of the Ti adhesion layer.) They were then washed in 18-MΩ $H_2O$ and can be stored for up to 2 h in ambient before use. At the point of use, the substrates were checked again by $H_2O$ immersion to confirm from uniform wetting that the surface is molecularly clean (hydrophilic).

**Molecular Assembly.** The first step is to assemble 1-hexadecanethiol (HDT) on the Au surface by immersing in 5 mM toluene solution at 22 °C for 10 min and rinsing twice with clean toluene. The next step is to assemble 3-aminopropylsilyloxane (APS) on the exposed $SiO_2$. There are numerous literature procedures,[10,25−30] but most yield multilayer films that overcoat the passivated Au, leading to indiscriminate activation of the entire substrate toward electroless metallization. Furthermore, procedures that require refluxing solvent conditions are also unsuitable because the alkanethiols desorb from Au above 80−100 °C.[6,9,31] We found a suitable room-temperature vapor-phase alternative. The HDT-modified Au patterns were exposed to APS vapor for 4 h at 22 °C in a drybox. The equilibrium vapor pressure of APS is sufficiently high at ∼0.1 mmHg. APS is thought to first hydrogen bond[32] to the physisorbed surface $H_2O$ and Si−OH groups and then undergo slow hydrolysis and covalent bonding.[25,33]

Ellipsometry confirms the presence of an APS monolayer (measured after baking the substrates at 120 °C for 10 min). The change in the ellipsometric angle $\Delta(\Delta)$ of the $SiO_2$/Si substrate is $-2.7 \pm 0.2°$ ($\lambda = 633$ nm and $\theta = 70.0°$). This gives a film thickness of $10 \pm 1$ Å (assuming $n = 1.4 \pm 0.05$), which corresponds to a monolayer coverage, since the extended length of the APS group is ∼8.5 Å. For comparison, HDT does not bind to $SiO_2$ (expected, $\Delta(\Delta) = 0.0$; found, $+0.1 \pm 0.2°$). However, APS does bind to Au[28] but not to HDT-modified Au. Therefore, the sequence of HDT masking followed by APS priming is crucial.

In the same way, the surface can be fluorinated with 1,1,2,2-4*H*-perfluoroundecyltriethoxysilane (PFS) to give a $6 \pm 1$ Å thick film ($\Delta(\Delta) = -1.4 \pm 0.2°$, assuming $n = 1.3 \pm 0.05$). Since the extended length of the PFS group is ∼15 Å, this indicates submonolayer coverage with either high tilt angles and/or strong lateral disorder of the PFS. Nevertheless, the surface becomes strongly hydrophobic with a static water contact angle greater than 110°.

**Activation and Electroless Deposition.** To completely condense the APS monolayer film, it is usually heated above 100 °C[25,28,33] to render it water insoluble.[10,34] However, HDT is thermally labile, and so our substrates were not annealed but directly immersed (for 2 min) into a 17 mM 98:2 v/v EtOH/$H_2O$ solution of $PdCl_2$ stabilized with 20 mM HCl, followed by dip washing in three separate 95:5 EtOH/$H_2O$ baths. The Pd bath was prepared by dissolving $PdCl_2 \cdot 6H_2O$ into absolute EtOH acidified with the required amount of concentrated HCl on a hot plate. The APS monolayer survived the treatment, perhaps because complexation with Pd(II) breaks the intramolecular hydrogen bonding[25,32,33] to trigger complete condensation of the silanol groups. These substrates were then dipped into an electroless Ni bath (pH ≈ 4−5) maintained at 90 °C to deposit an alloy of Ni with a few percent of P. This bath was prepared from stock solutions of 24 mL of EN4024 A and 45 mL of EN4024 B (Fidelity) and 230 mL of $H_2O$. Immersion times between 10 and 60 s were used to compensate for the variable induction time. The complexed Pd(II) is reduced by the bath to Pd(0) clusters, which are thought to be the active species for catalyzing electroless deposition.[22,35]

## Results and Discussion

The selectivity and mutual compatibility of the molecular masking, priming, and activation steps are crucial to the strategy. The results summarized in Table 1 confirm that these can be achieved within the overall framework depicted in Scheme 1.

Selected scanning electron micrographs (SEMs) of the cleaved edge of these structures are shown in Figure 1. To interpret these images, Au appears brighter than Ni, owing to the higher secondary electron yield of Au. Also, as Au is more ductile than the deposited Ni, the cleaved edge of Au exhibits significant pullout in contrast to the smooth fracture of the Ni edge.

The pristine surface of Au is smooth with the typical 100-nm rolling hill-lock features (Figure 1a). This surface is able to catalyze Ni(II) reduction, and thus Ni metallization occurs exclusively on the Au surface (Figure 1b). Au passivated with a monolayer of HDT loses this catalytic activity, and thus Ni does not nucleate even after 1 min in the bath (Figure 1c). See also entries 5 and 6 in Table 1. Large area optical and electron microscopy confirm that no Ni grains are found.

The Pd-activated APS assembled on $SiO_2$ does locally catalyze Ni(II) reduction to fine Ni grains (Figure 1d). Compare entries 3, 4, and 6 in Table 1. The HDT protection time on Au in the hot acidic Ni bath is >1 min. During this time, the bound Pd species successfully catalyzes the

(24) Moberg, P.; McCarley, R. L. *J. Electrochem. Soc.* **1997**, *144*, L151−L153.
(25) de Haan, J. W.; Bogaert, V. D.; Ponjeé, J. J.; van de Ven, L. J. M. *J. Colloid Interface Sci.* **1986**, *110*, 591−600.
(26) Britcher, L. G.; Kehoe, D. C.; Matisons, J. G.; Smart, R. S. C.; Swincer, A. G. *Langmuir* **1993**, *9*, 1609−1613.
(27) Kallury, K. M. R.; Macdonald, P. M.; Thompson, M. *Langmuir* **1994**, *10*, 492−499.
(28) Kurth, D. G.; Bein, T. *Langmuir* **1995**, *11*, 3061−3067.
(29) Moon, J. H.; Kim, J. H.; Kim, K.-J.; Kang, T.-H.; Kim, B.; Kim, C.-H.; Hahn, J. H.; Park, J. W. *Langmuir* **1997**, *13*, 4305−4310.
(30) Ho, P. K. H.; Granström, M.; Friend, R. H.; Greenham, N. C. *Adv. Mater.* **1998**, *10*, 769−774.
(31) Bumm, L. A.; Arnold, J. J.; Charles, L. F.; Dunbar, T. D.; Allara, D. L.; Weiss, P. S. *J. Am. Chem. Soc.* **1999**, *121*, 8017−8021.
(32) Piers, A. S.; Rochester, C. H. *J. Colloid Interface Sci.* **1995**, *174*, 97−103.
(33) Chiang, C.-H.; Ishida, H.; Koenig, J. L. *J. Colloid Interface Sci.* **1980**, *74*, 396−404.
(34) Vandenberg, E. T.; Bertilsson, L.; Liedberg, B.; Uvdal, K.; Erlandsson, R.; Elwing, H.; Lundström, I. *J. Colloid Interface Sci.* **1991**, *147*, 103−118.
(35) Jackson, R. L. *J. Electrochem. Soc.* **1990**, *137*, 95−101.

**Table 1. Catalytic Activity of Various Surface-Modified Substrates toward Electroless Ni Metallization[a]**

| | pretreatment | observation | conclusion |
|---|---|---|---|
| 1 | blank (no Pd(II) treatment) | Ni deposits on Au but not on $SiO_2$ after 5 s see Figure 1b | confirms catalytic activity of Au surface toward electroless Ni |
| 2 | HDT-treated (no Pd(II) treatment) | Ni does not deposit on Au even after 40 s see Figure 1c | passivation of Au by HDT even under electroless Ni bath conditions |
| 3 | (i) APS-treated (ii) Pd(II)-treated | Ni deposits rapidly on Au and extends over $SiO_2$ | activation of $SiO_2$ to electroless Ni with Pd(II)−APS |
| 4 | (i) HDT-treated (ii) APS-treated (iii) Pd(II)-treated | Ni deposits preferentially on $SiO_2$ but not on Au see Figures 1d and e and 2c and d | simultaneous activation of $SiO_2$ and passivation of Au |
| 5 | (i) HDT-treated (ii) PFS-treated (iii) Pd(II)-treated | Ni does not deposit even after 60 s | passivation of Au by HDT and no activation of $SiO_2$ by PFS |
| 6 | (i) PFS-treated (ii) Pd(II)-treated | Ni deposits on Au after 40 s, but not $SiO_2$ | no passivation of Au by PFS and no activation of $SiO_2$ by PFS |

[a] HDT = 1-hexadecanethiol, APS = (3-aminopropyl)triethoxysilane, PFS = 1,1,2,2-4*H*-perfluoroundecyltriethoxysilane.

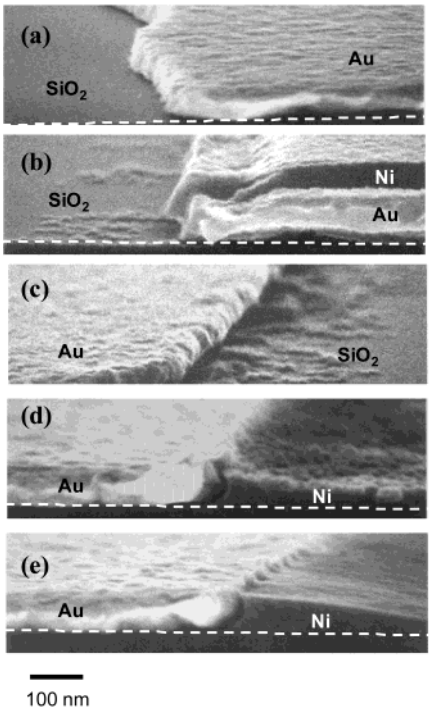


**Figure 1.** Scanning electron micrographs of cross sections of the Au−Ni junction. See Table 1 for explanations for the experiments.

selective deposition of electroless Ni over the exposed $SiO_2$ region. However, the APS film has limited hydrolytic stability in the Ni bath and will dissolve away if induction does not occur within ~20 s. If induction does occur within this time, the deposited Ni film does pass the Scotch tape peel test, which indicates good adhesion to the substrate.

The Ni grains appear to nucleate and grow from the Au sidewall, as evidenced by the larger thickness there, and extend over the $SiO_2$ substrate but not over the Au surface itself, at least for the early stages of Ni film nucleation and growth. The Au−Ni metallurgical junction along the top surface appears to be rough at the 10-nm length scale with apparent contact between the Ni and Au, limited by an instrument resolution of 3−5 nm. The fact that Ni does deposit even under a convex-shaped Au sidewall to form the complementary shape suggests that it is conformal to the sidewall, and the apparent gap in some images is therefore an artifact of ductile pullout of Au. At a later stage of growth, the Ni film thickness increases and its morphology becomes smoother (Figure 1e). The thickness of the HDT monolayer (~2 nm) cannot be resolved in these micrographs.

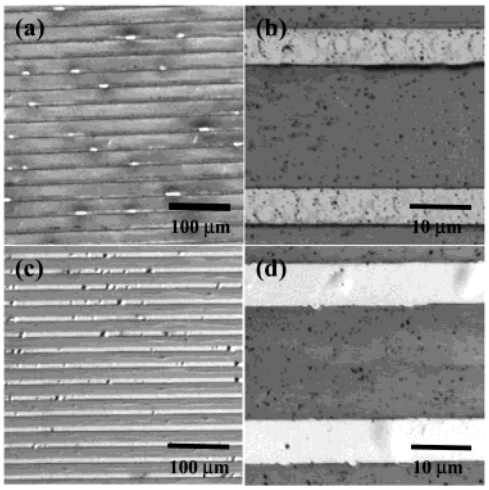


**Figure 2.** Optical micrographs of substrate test patterns. Parts a and b are Ni metallization without the Au passivation step, while parts c and d are done with the Au passivation step. The spots and haze in parts b and d are the characteristic signature of nodular Ni film growth. In parts c and d Ni does not deposit on the Au, which retains a clean look in these images.

Figure 2 shows the optical images that provide a larger scale view of the electroless deposition process. Parts a and b of Figure 2 show that, without the Au passivation step (but retaining the APS priming and Pd activation steps), electroless Ni grows all over the substrate to give a dull nodular appearance over both the Au and $SiO_2$ regions. Parts c and d of Figure 2 show that, by incorporating the Au passivation step, electroless Ni is spatially confined to the activated $SiO_2$ region. The Au lines remain bright and clean. Also, the contact line for films growing simultaneously from facing Au sidewalls is visible in Figure 2c. Therefore, the necessary selective destabilization of the electrochemical cell to initiate and sustain Ni(II) reduction over selected areas can be well-controlled over millimeter-scale areas with feature sizes down to the micron range by the appropriate surface modification in our experiments.

Two factors must be involved in the passivation of Au by HDT. The close-packed alkyl chains prevent ion permeation to the Au surface,[5] and so incipient reduction of Ni(II) has to occur outside a 2-nm-thick tunnel barrier, which weakens the electronic coupling. The adiabatic tunneling relation given by $j_{tunnel} \sim \exp(-\beta d)$, where $j_{tunnel}$ is the tunnel current, $d$ is the tunnel distance (in $CH_2$ units), and $\beta$ is an exponent $\approx 0.9/CH_2$,[36,37] predicts the exchange current density to be diminished by a factor of

(36) Closs, G. L.; Miller, J. R. *Science* **1988**, *240*, 440−447.

$10^{-6}$ compared to that for bare Au. Using a longer alkyl spacer will reduce this coupling even more. A second factor is the hydrophobicity of the HDT-modified Au, which raises the activation energy for Ni cluster attachment. These two factors together appear to sufficiently suppress the reduction of Ni(II) over the passivated Au surface at the electroless deposition potential[1] that is set up across the substrate surface. This potential is common to both the Au and $SiO_2$ surfaces because electrostatic potential coupling occurs through the intervening thin native oxide layer.

Finally, the binding of Pd(II) to APS is complicated by a complex equilibria involving $Cl^-$ and $H_2O$ to give various mono- and polynuclear species. A relatively high critical surface threshold concentration has been thought to be necessary for activation.[22,35] For a pH of ~1.7, a $[Cl^-]$/[Pd(II)] ratio of 3.2, and 2% $H_2O$ in EtOH, as in our experiments, the predominant monomeric species could be either $PdCl_3(H_2O)^-$ or $PdCl_3(EtOH)^-$.[38−40] Nevertheless, the results obtained here suggest that sufficient quantities of Pd(II) can be bound within minutes to an APS monolayer to activate electroless Ni deposition. Furthermore, our Pd(II) solution can be used for several weeks after preparation and appears to be more stable against bulk hydrolysis than the $PdCl_4^{2-}$ solution with near neutral pH values.[22]

## Conclusions

In summary, we have developed an orthogonal electroless metal patterning scheme by assembling first a 1-hexadecanethiol monolayer on Au in a solution process and then a 3-aminopropylsiloxane monolayer on the adjacent $SiO_2$ substrate region via a vapor-phase process. Activation of the aminosilane with Pd(II) followed by electroless Ni deposition produces self-aligned lateral metal thin-film structures that are essentially conformal. With further refinement of the self-assembly and electroless chemistry, we expect a wide range of orthogonal metal systems can be implemented. The approach can be further combined with deep-UV lithography,[41] microcontact printing of the activating species,[20,42,43] or chemical vapor deposition.[44,45]

**Acknowledgment.** We thank L.-L. Chua for useful discussions of the SEM images. P.K.H.H. is partially supported by a Research Fellowship from St John's College (Cambridge, U.K.) for the duration of this work and is on leave from the National University of Singapore (Singapore).

LA0260988

(37) Miller, C.; Cuendet, P.; Grätzel, M. *J. Phys. Chem.* **1991**, *95*, 877−886.
(38) *Handbook of metal−ligand heats and related thermodynamic quantities*, 2nd ed.; Marcel Dekker: New York, 1976.
(39) *Stability constants of metal-ion complexes: Part B Organic Ligands*; Pergamon Press: New York, 1979.
(40) *Critical stability constants*; Plenum Press: New York, 1982.
(41) Dulcey, C. S.; Georger, J. H., Jr.; Krauthamer, V.; Stenger, D. A.; Fare, T. L.; Calvert, J. M. *Science* **1991**, *1991*, 551−554.
(42) Hidber, P. C.; Helbig, W.; Kim, E.; Whitesides, G. M. *Langmuir* **1996**, *12*, 1375−1380.
(43) Kind, H.; Geissler, M.; Schmid, H.; Michel, B.; Kern, K.; Delamarche, E. *Langmuir* **2000**, *16*, 6367−6373.
(44) Jeon, N. L.; Clem, P. G.; Payne, D. A.; Nuzzo, R. G. *Langmuir* **1996**, *12*, 5350−5355.
(45) Jeon, N. L.; Lin, W.; Erhardt, M. K.; Girolami, G. S.; Nuzzo, R. G. *Langmuir* **1997**, *13*, 3833−3838.